9-1. Research Divisions
Division for Integrated Studies

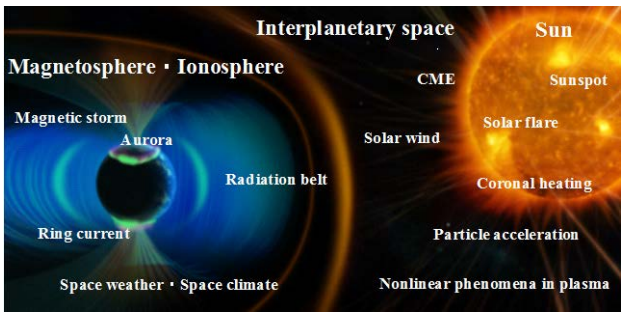

Research topics and keywords

- Solar flare · CME
- Inner-magnetosphere · Radiation belt
- Aurora substorm
- Space weather · Space storm
- Space climate · Long-term variations of the Sun
- Space plasma
- Computer simulation
- Data assimilation

Introduction to Division for Integrated Studies

The solar–terrestrial environment is a complex system that consists of nonlinear, non-equilibrium, and multi-scale interacting processes. The research activities in the Division for Integrated Studies are aimed at understanding the mechanisms and predicting the dynamics of various phenomena in the solar–terrestrial environment through data analyses and modeling studies. Some of the major results are introduced below.

Main Achievements in FY2017

1. Nonlinear dynamics of a solar eruptive flux rope

A magnetohydrodynamic (MHD) simulation was conducted to investigate the nonlinear dynamics of a solar eruptive flux rope. The simulation showed that the eruptive flux tube accelerates rapidly even though it passes through a region predicted from a theoretical model where the evolution of a flux rope should be suppressed. We found that the nonlinear interaction of the flux rope evolution and reconnection, which is not taken into account in the theoretical model, plays an important role in accelerating the flux rope. These results were summarized in Inoue et al. *Nature Communications* 9, 174 (2018).

2. Numerical study of prominence eruptions with radiative cooling condensation

As part of the Project for Solar-Terrestrial Environment Prediction (PSTEP), we reproduced solar prominence eruption, a progenitor of coronal mass ejection, using a MHD simulation including thermal conduction and radiative cooling. In this study, we combined a prominence formation model (Kaneko & Yokoyama, 2017) and a flare trigger model (Kusano et al., 2012), and investigated the impact of radiative condensation on prominence eruption. We found that momentum in the corona as well as mass is condensed into prominence, facilitating initiation of the MHD instability responsible for eruptions. We also found that prominence oscillates before eruption, as suggested by previous observations.

3. Study on the onset mechanism and prediction of solar explosions

To understand the mechanism of solar explosions, i.e., solar flares and coronal mass emissions, and devise a new scheme to predict these, we analyzed the evolution of the parameter κ^*, which is a proxy for the critical parameter for the double-arc instability (DAI) that was recently predicted to be the initial driver of solar eruptions by Ishiguro and Kusano (2017). We calculated κ^* for solar active region NOAA 11158 using vector magnetic field data observed by the Solar Dynamics Observatory (SDO) satellite and the nonlinear force-free field model. We found that κ^* increased to greater than a certain level before the two major flares and decreased drastically just after the flares. These results support the

theoretical model in that the DAI plays a crucial role in triggering solar eruptions, and suggests the applicability of the nonlinear force-free model for predicting the onset of solar eruptions.

4. Statistical study of the relationship between flare activity and magnetic structure in solar active regions

Study of the magnetic field in solar active regions is important for understanding the physics of solar flares. At present, the relationship between flare occurrence and energy storage in the coronal magnetic field in active regions is not well understood because coronal field observations are difficult. We reconstructed configurations of the coronal magnetic field from observational data of the surface magnetic field using a non-linear force free field model for a number of active regions from June 2010 to February 2016, and conducted a statistical study on flare activity and energy storage in the coronal magnetic field. The analysis showed that flare activity has a better correlation with the magnetic twist than with the energy excess from the potential energy state in the active region magnetic field. We also created a catalogue of coronal magnetic parameters for more than 100 active regions.

5. Statistical study of active-region microflares observed with Hinode/XRT

The solar corona, the outermost atmosphere of the Sun, is very hot (~ 1 MK) compared with its surface (~6,000 K) ; this is one of the major unsolved problems in solar physics. Small solar flares such as microflares and nanoflares are one possible source of the heating mechanism in the solar corona. Using X-ray Telescope (XRT) on board Hinode, we succeeded in detecting a very large number of microflares in an active region, and found that the energy distribution of microflares can be described by a power-law ($dN/dE\ A \times E^{-\alpha}$), with α greater than 2. This result means that the total energy of very small flares is sufficient to heat the active-region corona if the distribution extends to the lower energy range with the same α value.

6. Investigation of thermal response in wave-heated corona loops

We conducted 3D MHD simulations to investigate the thermal response in wave-heated corona loops. As a result of random forces on the foot point of the loop, MHD waves are excited to transport their energy to the upper atmosphere, and the resultant MHD waves become non-linear to transport their energy to smaller spatial scales. As a natural consequence of energy dissipation, we demonstrated that a 1 MK corona would be produced and, in addition, collision between counter propagating Alfven waves in the corona causes an impulsive temperature increase. These facts demonstrate that wave-heating mechanisms are able to produce nano-flare like events, as the heating is spatially localized and temporally intermittent.

7. Numerical study on the regional difference of solar chromospheric jets

We investigate the regional difference of solar chromospheric jets using the numerical simulation. The MHD equations with the effects of gravity, radiative energy transport, latent heat of ionization, and field-aligned thermal conduction are numerically solved for the realistic modeling of the solar chromosphere. We assume that the regional difference is characterized by two parameters: the photospheric magnetic field imbalance and the coronal temperature. We mimic the quiet and active regions on the Sun by choosing the two parameters of the simulation. The simulated thermal convection self-consistently excites various MHD waves, which are the energy sources of the chromospheric jets. The resultant numerical simulation shows the regional difference of simulated chromospheric jets quantitatively consistent with the observation. This regional difference of the simulation is naturally explained by the nonlinear amplification of the Alfven wave. Our results indicate that the Alfven wave plays a crucial role in the formation process of solar spicules.

8. Next solar cycle prediction study

We developed a surface flux transport (SFT) model and conducted calculations to predict activity in the next solar cycle. We obtained the result that the next cycle will be weaker than the current solar cycle by a few 10% (Iijima et al. 2017, *Astron. Astrophys.*). To achieve a more precise prediction, the long-term variation of the solar surface velocity was analyzed from the observations, and we also clarified the relationship between the observed velocities and the magnetic field strength.

9. Simultaneous observation of auroral substorm onset in Polar satellite global images and ground-based all-sky images

Substorm onset was originally defined as a longitudinally extended sudden auroral brightening ("Akasofu initial brightening"), which is followed a few minutes later by an auroral poleward expansion in ground-based all-sky images. In satellite-based global images, however, this clearly marked two-stage development has not been evident and, instead, substorm onsets have been identified as localized sudden brightenings, which immediately expand poleward. To resolve these differences, optical substorm onset signatures in global images and all-sky images were compared for a substorm that occurred on December 7, 1999. The all-sky images revealed the two-stage Akasofu initial brightening (2124:50 UT) and the subsequent poleward expansion (2127:50 UT), whereas the global images revealed only an onset brightening that started at 2127:49 UT. Thus, the onset in global images was delayed relative to the Akasofu initial brightening and, in fact, agreed with the poleward expansion in the all-sky images. The fact that the Akasofu initial brightening was not evident in the global images may possibly be attributed to the limited spatial resolution of global images for thin auroral arc brightenings. The implications of these results for the definition of substorm onset are discussed herein.

10. Study of the dayside magnetic reconnection with MMS spacecraft data

We analyzed the structure and physical processes near the magnetic neutral line for the magnetic reconnection at the Earth's dayside magnetopause by applying the two fluid equations to the data obtained by MMS spacecraft. It was shown that there is a strong correlation between the magnitude of the electron collision term resulting from the electron-wave interactions and the intensity of the low frequency hybrid waves in the ion diffusion region that surrounds the magnetic neutral line. This strongly suggests the presence of anomalous resistivity due to excited waves.

11. Direct evidence of the pitch angle scattering of energetic electrons observed by ERG (Arase)

The ERG (Arase) satellite that was launched in December 2016 has an electron detector with high-angular resolution. In March 2017, there was a good conjugate observation between ERG and ground-based optical imagers in Canada, and active pulsating aurora was observed. During the period, ERG observed intense chorus emissions near the magnetic equator and identified for the first time the flux modulation inside the loss concurrently with the chorus variations. The pitch angle scattering by plasma waves in space has not been identified until this observation. The amplitude modulation of the pulsating aurora shows good correspondence with the flux modulation of electrons inside the loss cone, which shows the definitive evidence on the origin of the pulsating aurora. This result was reported in Nature as the first observational result of the ERG project.

12. Rapid acceleration of MeV electrons associated with sudden commencement

We investigated relativistic electron accelerations associated with SC with a code coupling simulation of global MHD and test-particle simulations. Results indicate wide energy electron accelerations through interactions between the fast mode waves and drifted electrons.

13. Quasi-periodic modulations in energetic electrons without corresponding ULF waves observed by ERG satellite

ULF waves affect energetic electrons in the radiation belt. To understand the spatial properties of energetic electrons, we compared the energetic electron flux modulations observed by the Radiation Belt Storm Probes (RBSP) and ERG satellites with the longitudinal distance. RBSP and ERG simultaneously observed relativistic electron flux modulations with frequency in the dusk and dawn sectors, respectively. From the dispersion signature, we estimated the source regions of the flux modulations and found that the source regions were located in the dusk-noon sector. ULF waves observed in the dusk sector did not appear in the dawn sector and these ULF waves might generate electron modulations in the dusk-noon sector, which may then drift eastward and be observed by ERG.

14. Direct evidence of the nonlinear interactions of electromagnetic ion cyclotron waves by spacecraft observation

Nonlinear interactions by electromagnetic ion cyclotron (EMIC) waves have an impact over a wide energy range of ions and relativistic electrons. We developed a method to detect these interactions directly from THEMIS spacecraft data. Calculating the phase difference between the wave electromagnetic fields and particle velocities, we obtained the distribution of the ions over phase angle, and the values indicating the nonlinear resonant currents. We obtained evidence of energy transfer from the energetic ions to the EMIC waves with increasing frequency.

15. Statistical analysis of EMIC waves observed by Plasma Wave Experiment aboard Arase

The Plasma Wave Experiment (PWE) is one of the scientific instruments onboard the ERG satellite that measures the electric and magnetic fields in the inner magnetosphere. One significant advantage of ERG observations is the broad latitudinal coverage because of the orbital inclination of ERG is 31 degrees, and the observations in both around the geomagnetic equatorial region and around the mid-latitude region are possible.

We successfully obtained 166 EMIC waves during the first 9 months after the satellite was launched, and found that 37% of observed EMIC waves obtained by the PWE had fine structures. Our statistical analyses showed that the spatial distributions of the unstructured EMIC waves and of the fine-structured EMIC waves were significantly different. The wide latitudinal coverage of Arase's orbit enabled this unique analysis.

16. Non-MHD effects in the Rayleigh-Taylor instability

The nonlinear evolution of the Rayleigh-Taylor instability (RTI) at a density shear layer transverse to the magnetic field in a collisionless plasma was investigated using a fully kinetic Vlasov simulation with two spatial and two velocity dimensions. The primary RTI in the MHD regime develops symmetrically in a coordinate axis parallel to gravity, as seen in the previous MHD simulations. The primary RTI in the Hall-MHD regime develops asymmetrically in a coordinate axis parallel to gravity. A compressible flow is formed at the secondary density shear layer by the Hall effect, which generates a strong scalar pressure gradient of ions, and a Hall electric field due to the diamagnetic current results in an asymmetric flow at the tip of the finger structure. In the primary RTI with the ion gyro kinetic effect, a secondary RTI with a wavelength shorter than the wavelength of the primary RTI is generated at the saturation stage of the primary RTI. A seed perturbation for the secondary RTI is excited by another secondary instability due to the coupling between the electron stress tensor and the Hall electric field. The heat flux term plays an important role in the time development of the total pressure. In contrast, the contribution of the ion stress tensor to both the electric current and the total pressure is small.